1

Modeling Control of VSCs

1.1. Introduction

In recent years, the technical possibility has matched the market opportunity given that the National Energy Policies (associated with the exploitation of renewable energy sources) and the Electricity Sector Reforms (deregulation) demand higher efficiencies, such as power flow (PF) control capabilities and growing interconnections, with asynchronous features for more economic or reliable system operation.

Under this scenario, the widely deployed alternating current (AC) transmission technology presents limitations, since higher efficiencies, PF control capabilities and growing interconnections with asynchronous features are required for a more economical and reliable system operation [HAM 00]. Moreover, the long-distance bulk-power transmission and the synchronous connections between AC networks are claimed to deteriorate the overall dynamic behavior of the AC systems, while the submarine cable crossing length is limited by the management of the reactive power [HAM 00].

These applications among others, together with the development of power semiconductors, microprocessors and new insulation materials, have spurred the advancement of high voltage direct current (HVDC) technology as an alternative for power transmission [BAH 07], notwithstanding the technological challenges that remain, such as the improvement of Direct Current (DC) breakers and cables rating.

More recently, the advent of the high-power insulated gate bipolar transistor (IGBT) and its turn-off capability has given rise to a new converter technology: the voltage source converter (VSC) or forced-commuted converter (FCC) that is capable to provide reactive power support and control the active PF, the reason why it is considered to outmatch its predecessor, the well-known current source converter (CSC) or line-commuted converter (LCC) [FLO 09].

Traditionally, when considering an HVDC link, only two converters are taken into account, connected through a DC cable. In this scenario, significant research has been carried out, such as [BAJ 08a] and [BON 06]. A basic configuration of a VSC-based HVDC transmission system is presented in Figure 1.1, where the converter is represented by a six-pulse bridge equipped with self-commutating switches and diodes connected in antiparallel.

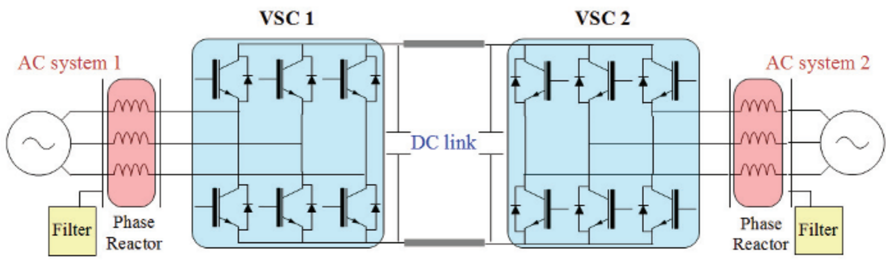

Figure 1.1. *Two-terminal VSC system*

It is worth mentioning that this point-to-point connection may be achieved using both aforementioned technologies (CSC and VSC). Nevertheless, an outstanding difference, from the control point of view, appears. When thyristor-based converters (CSC) are used, only one degree of freedom is available at each terminal and its operating principle is based on keeping a constant DC current (reason why it is called CSC), while both magnitude and direction of the PF are controlled by changing the magnitude and direction of DC voltage as the control system acts through firing angle adjustments of the valves and through tap changer adjustments on the converter transformers [BAJ 08a]. Thus, the power reversal in CSC-based HVDC links is obtained by reversing the polarity of the direct voltages at both ends, which represents an issue when considering multi-terminal operation [BAJ 08a].

In contrast, VSC converters offer two degrees of freedom at each terminal, which allows the independent control of the active and reactive power. Moreover, each converter can be used to synthesize a balanced set of three phase voltages like inertia-less synchronous machine, provided that the DC voltage is free from oscillations during disturbances and fault occurrences on the AC sides of the VSC-HVDC stations [HAI 08].

Furthermore, unlike conventional HVDC transmission (CSC), the transistor-based converters (VSC) themselves have no reactive power demand and can actually control their reactive power to regulate AC system voltage. The dynamic voltage support of the AC voltage offered at each VSC terminal improves the voltage stability and can increase the transfer capability of the sending and receiving AC systems without much need for AC system reinforcement.

Moreover, the PF direction in the VSCs is controlled by changing the direction of the current, which makes them suitable for multi-terminal operation.

In this chapter, modeling and control of VSC converter will be addressed taking into account future conditions and constraints for multi-terminal configuration.

1.2. Steady state voltage control systems – multi-terminal direct current (VSC-MTDC) model

The steady state of a system refers to an equilibrium condition, where the effect of transients is no longer relevant. In power systems, any specific steady state operating point can be determined through an analytical technique called PF analysis (also known as load-flow), where the loads are modeled as bulk power delivery points and the voltages of the transmission network can be determined [KUN 94].

An analogous study for a VSC-MTDC system was conducted in [BEE 12]. The DC power flow (DC PF) calculation can be used to find the starting point for dynamic analysis, considering that the VSC-MTDC system is operating under a centralized DC voltage control such as master/slave (M/S), where only one converter (known as slack converter) is designated to keep the DC voltages in a close band around its rated value through active power compensation.

Once more, an outstanding difference between the AC and DC systems must be kept on sight. In an AC transmission system, where the line resistances are neglected given the inductance higher values, the active PF is dominated by the angle differences between different buses, while the reactive PF is mainly associated with the voltage magnitude deviation of different nodes [KUN 94].

When considering a DC grid, there is no reactive PF; therefore, the PF calculation is solely concerned with the active power, which, contrary to the AC case, is dictated by the differences in the voltage magnitudes between the different nodes. Another specification of the DC grid is the absence of the frequency; hence, only resistances are introduced in the nodal admittance matrix (Y_{dc}).

In the following, the selected sign convention is defined. Afterward, the DC side model is built, followed by the DC PF calculation. Then, the steady state AC side model is presented, where the filter and other station equipment are not considered, and the VSC is represented by its average model, approximation consistent with the phenomena of interest. Finally, control structures of VSC converters for multi-terminal DC grids taking into account normal as well as disturbed operations will be proposed. For the sake of understanding, vector control method will be used with adequate references.

1.2.1. *Convention*

DC power and current are assumed to be positive when they are flowing away from the VSC, as shown in Figure 1.2. Therefore, DC power (and current) are considered as positive when they are being injected into the DC grid.

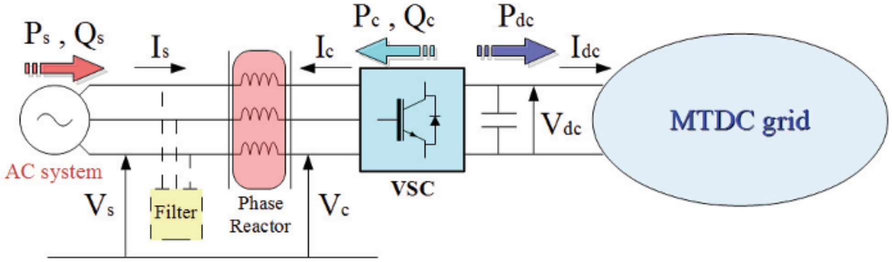

Figure 1.2. *Power and current directions*

1.2.2. *DC side model*

In steady state, the DC network is modeled by the link resistances (R_{ij}). It is a common practice to add a shunt resistance to represent the converter losses as shown in Figure 1.3.

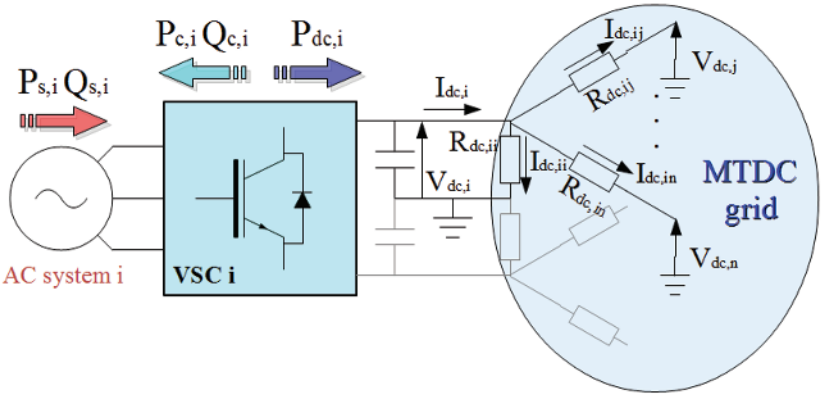

Figure 1.3. *Monopolar symmetrically grounded VSC-MTDC system*

In a MTDC system of *n* DC nodes, the current injected in a node *i* is calculated as the sum of all the currents flowing to the other (*n-1*) interconnected nodes and the current going into the shunt resistance ($R_{dc,ii}$), as written in equation [1.1].

$$I_{dc,i} = \left(\sum_{\substack{j=1 \\ j \neq i}}^{n} \frac{1}{R_{dc,ij}} \cdot (V_{dc,i} - V_{dc,j}) \right) + \frac{V_{dc,i}}{R_{dc,ii}} \qquad [1.1]$$

1.2.3. *DC power flow calculation*

The active power in each node is the product of its DC voltage and DC current. For a monopolar symmetrically grounded converter, as the one shown in Figure 1.3, and for bipolar converters the power injection is given by equation [1.2].

$$P_{dc,i} = 2V_{dc,i} I_{dc,i} \qquad [1.2]$$

Substituting equation [1.1] into [1.2], it is possible to calculate the power injection into each DC node, when the DC voltage values are known beforehand as shown in equation [1.3].

$$P_{dc,i} = 2V_{dc,i} \cdot \left(\left(\sum_{\substack{j=1 \\ j \neq i}}^{n} \frac{1}{R_{dc,ij}} \cdot (V_{dc,i} - V_{dc,j}) \right) + \frac{V_{dc,i}}{R_{dc,ii}} \right) \quad [1.3]$$

However, in a VSC-MTDC system under a centralized DC voltage control (M/S), the DC voltage is only known for the slack converter, while it remains as an unknown in the other nodes where the VSCs are operating in a constant active power injection mode ($P_{dc,i}$ known); giving rise to a nonlinear equations system that should be rewritten as equation [1.4].

$$Y_{dc} \mathbf{V_{dc}} - \left[\frac{P_{dc,i}}{2V_{dc,i}} \right] = 0 \quad [1.4]$$

where Y_{dc} is the DC nodal admittance matrix, since

$$\mathbf{I_{dc}} = Y_{dc} \mathbf{V_{dc}} \quad [1.5]$$

The solution of the equation system given in equation [1.4] gives the power injection at the slack converter and the DC voltages of all the VSCs operating in a constant active power injection mode. Therefore, after performing the DC power flow (PF), the voltage and active power injection of all the DC nodes in the MTDC grid will be perfectly specified.

1.2.4. *AC side model*

VSC converters are considered to be connected to the AC system through a phase reactor as shown in Figure 1.4. It is a common practice to include a transformer, but for the purposes of this study (where filters and other station equipment are not model), its representation is omitted.

The phase reactor is represented by a resistance (R_{pr}) and an inductance (L_{pr}). In the following, the perunit system is adopted as defined. The basic equation of this circuit, following the Kirchhoff's voltage law (KVL), is:

$$V_c - V_s = R_{pr} I_c + L_{pr} \frac{dI_c}{dt} \qquad [1.6]$$

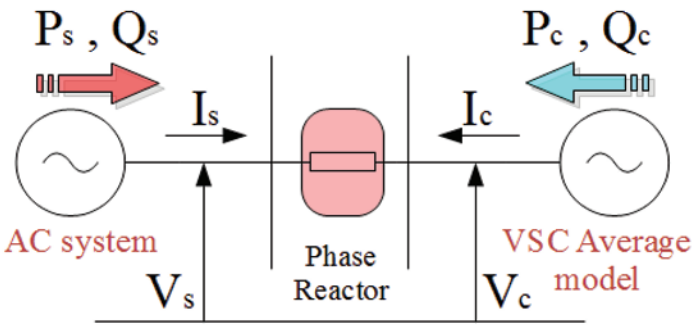

Figure 1.4. *Single-phase VSC representation*

HYPOTHESIS.–

– If a balanced three-phase system is considered, equation [1.6] can be transformed into a rotating *dq0* reference frame, using the Park–Clarke transformation (P) defined as:

$$P = \frac{2}{3}\begin{bmatrix} \cos(\theta) & \cos\left(\theta - \frac{2\pi}{3}\right) & \cos\left(\theta + \frac{2\pi}{3}\right) \\ -\sin(\theta) & -\sin\left(\theta - \frac{2\pi}{3}\right) & -\sin\left(\theta + \frac{2\pi}{3}\right) \\ \frac{1}{2} & \frac{1}{2} & \frac{1}{2} \end{bmatrix}$$

Such that, in steady state,

$$V_{cd} - V_{sd} = R_{pr} I_d - X_{pr} I_q \qquad [1.7]$$

$$V_{cq} - V_{sq} = R_{pr} I_q + X_{pr} I_d \qquad [1.8]$$

– Then, if the converter losses are not considered ($R_{ii} = \infty$),

$$P_c = -P_{dc} \qquad [1.9]$$

– And the phase reactor resistance and losses are neglected,

$$P_c = -P_s \qquad [1.10]$$

The active power at the system node and both sides of the VSC are the same.

– Moreover, if the AC system voltages (V_s) are considered as known (from the AC PF).

– The voltage-oriented control (VOC) method [TEO 11] is applied ($V_{sq} = 0$):

$$P_s = \frac{3}{2} V_{sd} I_{sd} \qquad [1.11]$$

$$Q_s = -\frac{3}{2} V_{sd} I_{sq} \qquad [1.12]$$

If the active and reactive powers injected by any AC system are defined as set points by the associated transmission system operators (TSO); then, the converter's AC side currents (I_d and I_q) can be determined by equations [1.11] and [1.12], since no filter is considered (thus, $I_s = - I_c$). Finally, the converter's AC side voltages (V_{cd} and V_{cq}) are given by equations [1.7] and [1.8].

1.3. Control system of VSC based on VOC

In response to the forthcoming massive renewable energy integration, which will be connected to the existing AC electrical network through power converters, great efforts have been devoted to the development of a greater performing control system that, alongside others, will contribute to mitigate the inherent problem of intermittent but clean renewable energy sources (RES).

In the literature, special attention has been given to the controllers design, including classical proportional integral (PI), hysteresis regulators and the development of customized adaptive algorithms [MIL 13, CHA 13]. Also, robust nonlinear control techniques based on Lyapunov and backstepping methodologies have been proposed, in which the system decoupling is obtained via a cascade structure and using the inherent time scales of the studied system [ELO 06]. Finally, the dead-beat (DB) control including current and voltage limitations has been suggested when high dynamic response is mandatory [BEN 04].

Additionally, available control methods have been evaluated for Voltage Source Converter (VSC)-HVDC transmission systems applications, such as direct power control (DPC) and vector control in different reference frames such as the VOC in *dq0* or alpha-beta [SOO 10]. However, in this study, the well-known closed-loop vector control method in conjunction with PI controllers in cascade structure is adopted according to [TEO 11], since this work aims to offer a contribution in the understanding of the overall VSC-MTDC system behavior in order to establish a DC voltage control philosophy, when further contributions regarding stability analysis as well as robustness properties to obtain effective control scheme can be subsequently included.

Therefore, in this section, only the control structure is presented, considering their integral and proportional gains as known. In practice, the inner (current) loop was tuned according to "modulus optimum" technique, while the outer (power/voltage) loop was tuned following the "symmetrical optimum" criteria as suggested in [BAJ 08b].

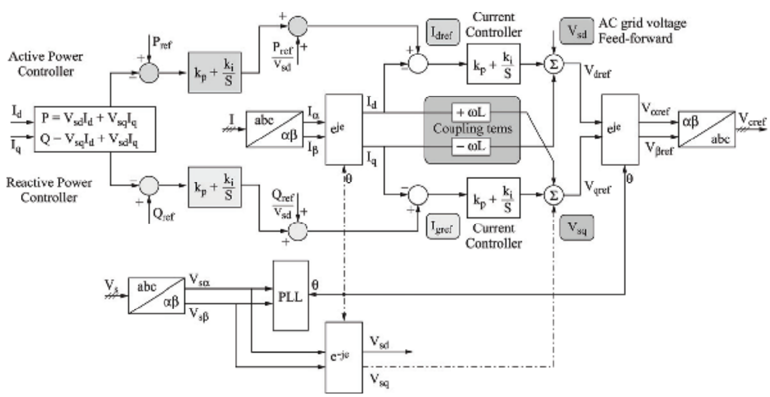

Figure 1.5. *PQ closed-loop VOC implemented on the dq synchronous frame*

The active and reactive power control structure, based on a closed-loop structure under synchronous frame VOC, is shown in Figure 1.5, as presented in [TEO 11], where PI-based controllers decide the reference current d and q components from the error between the actual injected powers and their reference values, resulting in a four loops control structure.

1.3.1. *Inner current controller*

The converter's AC side current can be controlled by two parallel inner loops using PI controllers that transform the current errors into voltage signals as shown in Figure 1.6.

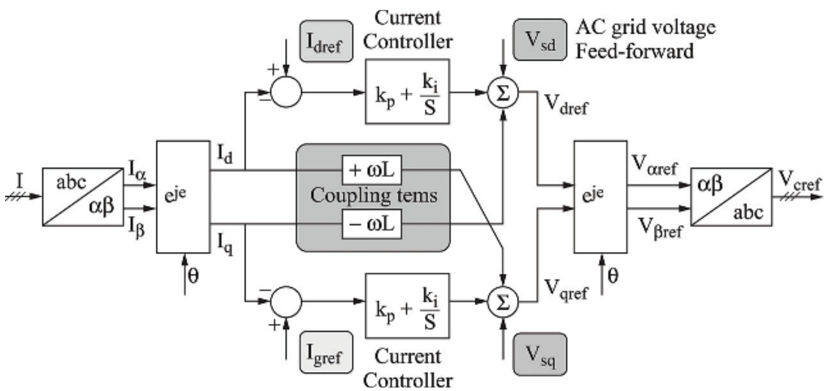

Figure 1.6. *Current controller structure – VOC based on dq synchronous frame*

The representative equation of the PI regulator is:

$$G_{PI}(s) = K_p + \frac{K_i}{s} = K_p\left(\frac{1+\tau_i S}{\tau_i S}\right) \qquad [1.13]$$

where the proportional gain K_p and integral time constant τ_i or the integral gain K_i are the design parameters calculated according to [BAJ 08b].

Using separate current controller loops for I_d and I_q, the converter reference voltage signals for the two axes (V_{dref} and V_{qref} in Figure I.6) are generated from the current error and the PI regulator transfer function.

$$V_{cdref} = \left(K_{p1} + \frac{K_{i1}}{s}\right)\left(I_{dref} - I_d\right) \qquad [1.14]$$

$$V_{cqref} = \left(K_{p1} + \frac{K_{i1}}{s} \right) \left(I_{qref} - I_q \right) \qquad [1.15]$$

In equations [1.16] and [1.17], the grid voltage has been feed-forwarded and the cross-coupling terms between the two control loops are added to compensate the ones introduced by the transformation to the rotating reference frame [TEO 11].

$$V_{cdref} = V_{sd} - \omega L_{pr} I_q + \left(K_{p1} + \frac{K_{i1}}{s} \right) \left(I_{dref} - I_d \right) \qquad [1.16]$$

$$V_{cqref} = V_{sq} + \omega L_{pr} I_d + \left(K_{p1} + \frac{K_{i1}}{s} \right) \left(I_{qref} - I_q \right) \qquad [1.17]$$

1.3.2. *Outer power controller*

An active and reactive power closed-loop control structure is employed; hence, the reference currents for the inner loop (I_{dref} and I_{qref}) are calculated in an outer power loop where the active and reactive powers injected are estimated using measurements (of three-phase voltages and currents) at the point of common coupling (PCC) and their values are compared to the set points.

Special attention must be given to the selected convention. If the power set points (P_{set_point} and Q_{set_point}) are defined by the TSO as injected by the AC system into the VSC station, while the controlled current (I_d and I_q) has been defined as injected by the VSC into the AC grid, the power reference value given to the control system (P_{ref} and Q_{ref} in Figure 1.5) must be defined in the same direction of the current, such that:

$$P_{ref} = -P_{set\_point} \qquad [1.18]$$

$$Q_{ref} = -Q_{set\_point} \qquad [1.19]$$

1.3.2.1. *Active power controller*

When the M/S DC voltage control strategy is implemented in a VSC MTDC system with an n DC nodes, $n - 1$ converters control the active power, and one controls the DC voltage. Therefore, the variable I_{dref} is calculated from the active power set point of all converters, except for the slack converter, through a combination of an open loop and a PI controller as expressed in equation [1.20]:

$$I_{dref} = \frac{P_{ref}}{V_{sd}} + \left(K_{pp} + \frac{K_{ip}}{s} \right) \left(P_{ref} - P \right) \qquad [1.20]$$

A feed-forward term representing the d-axis current (I_d) that should be generated when the injected power is equal to its reference is added to minimize the disadvantage of slow dynamic response of cascade control. Additionally, this contributes to improve stability since the load variation can be greatly reduced and, with it, the gain of voltage controller [BAJ 08b].

According to equation [1.11], it should be a 3/2 factor in the feed-forward term, but it has disappeared due to the chosen per unit system: the power and voltage bases have been set as the rated three-phase power of the converter [VA] and the peak value of rated line-to-neutral voltage [V].

1.3.2.2. *Reactive power controller*

Analogously, the q-axis current reference (I_{qref}) is calculated from the reactive power reference value (Q_{ref}), where a combination of an open loop and a PI controller is used to drive the reactive power to its desired value, leading to:

$$I_{qref} = -\frac{Q_{ref}}{V_{sd}} + \left(K_{pq} + \frac{K_{iq}}{s} \right) \left(Q_{ref} - Q \right) \qquad [1.21]$$

Alternatively to the reactive power, the magnitude of the AC grid voltage could be controlled; however, an extra control loop is needed to provide the reactive power reference to the reactive power control loop. In computer models, the reactive power injection necessary to keep the AC system's voltage in a given value can be calculated by an AC PF, where the converter is considered as a photo-voltaic (PV) node [KUN 94]. A sequential AC/DC PF has been proposed in [BEE 10a] and [BEE 10b].

In [COL 10], it is proposed to calculate the q-axis current reference directly from the voltage reference using a PI controller as in equation [1.22], but this scenario is not considered in this work since no further models of the AC grid have been so far included; thus, the evolution of the grid voltage (V_{sd}) in response to the control q-axis current is unknown.

$$I_{qref} = \left(K_{pv} + \frac{K_{iv}}{s} \right) \left(V_{acref} - V_{sd} \right) \quad [1.22]$$

1.3.3. *DC voltage controller*

1.3.3.1. *Master/slave DC voltage control*

When the M/S DC voltage control strategy is implemented, one converter of the VSC MTDC system controls the DC voltage. The control of the DC voltage could act directly on the d-axis reference current (i_{dref}) as shown in Figure 1.7. The design parameters of the controller are found through a linearization of the power equation [TEO 11]. Otherwise, in this work, the control of the DC voltage is considered to act on the DC current, here referred as i_{dcref}, and the d-axis reference current (i_{dref}) is found directly from the power balance equation, as represented in Figure 1.8. Therefore, a PI controller is used to keep the DC voltage of the slack converter at its reference value and the steady state DC current (as a function of the actual DC power injected by the slack converter into the DC grid, $P_{dc,slack}$, and the reference DC voltage) is feed-forwarded. Subsequently, the reference DC current of the slack converter can be expressed as:

$$I_{dcref,slack} = \frac{P_{dc,slack}}{2V_{dcref}} + \left(K_{pdc} + \frac{K_{idc}}{s} \right) \left(V_{dcref} - V_{dc,slack} \right) \quad [1.23]$$

where $P_{dc,slack}$ could be calculated using measurement at the DC bus [1.24], or, if the converter losses have been neglected, as a function of the calculated AC side converters voltage and current [1.25].

$$P_{dc,slack} = 2I_{dc,slack} V_{dc,slack} \quad [1.24]$$

$$P_{dc,slack} = -P_{c,slack} = -I_d V_{cd} - I_q V_{cq} \quad [1.25]$$

Finally, the d-axis reference current ($I_{dref,slack}$) is defined as:

$$I_{dref,slack} = -\frac{2I_{dcref,slack} V_{dc} + I_q V_{cq}}{V_{cd}} \quad [1.26]$$

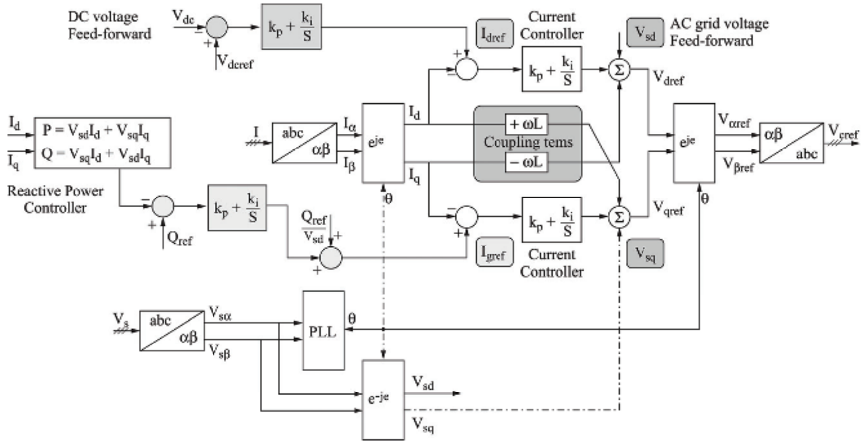

Figure 1.7. *V_{dc}-Q closed-loop VOC implemented on the dq synchronous frame*

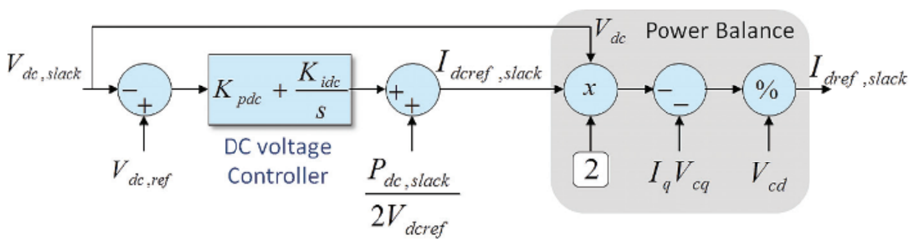

Figure 1.8. *DC voltage control structure*

1.3.3.2. *DC voltage: active power droop (VD)*

When the control of the DC voltage is considered to be distributed implementing a control strategy such as the DC voltage droop (VD), a group of converters may have a third control loop where the active power reference is generated as a function of a active *power set-point* (P_{dc0}) and the error between the actual DC voltage and its *set-point* (V_{dc0}) by a proportional controller, as shown in Figure 1.2, such that:

$$P_{ref\_droop} = P_{dc0} + K_{pd}\left(V_{dc0} - V_{dc}\right) \quad [1.27]$$

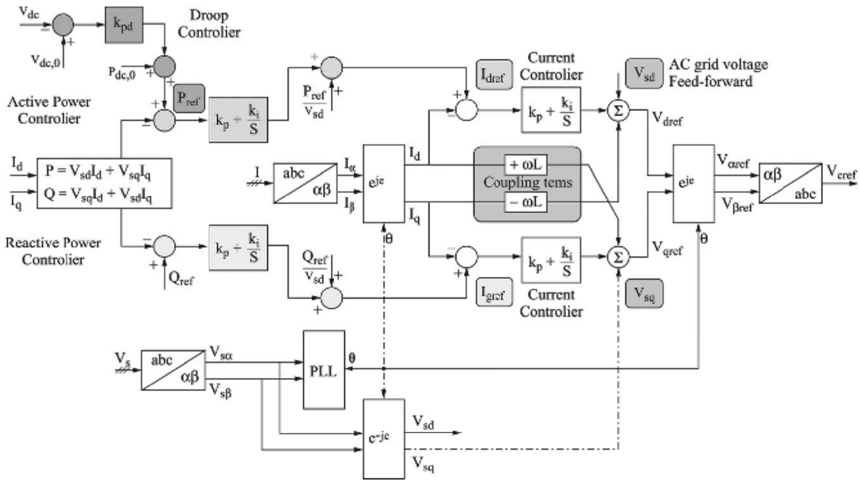

Figure 1.9. *DC voltage droop proportional controller*

1.4. Conclusion

In this chapter, having defined the adopted convention, the DC side model is built followed by the DC PF calculation (for more details see [CAR 12]). Then, the steady state AC side model has been presented, where the filter and other station equipment are not considered, thereafter the VSC has been modeled by its average model, approximation consistent with the phenomena of interest. Finally, control structures of VSC converter for multi-terminal DC grid taking into account normal as well as disturbed operations have been proposed considering only VOC method.